



ORIGINAL ARTICLE

Fluorescent sensor for *in-vivo* bio-imaging, precise tracking of Fe³⁺ ions in Zebrafish embryos and visual measuring of Cu²⁺ ions in pico-molar level



A. Senthil Murugan^a, M. Kiruthika^b, E.R. Abel Noelson^a, P. Yogapandi^b,
G. Gnana kumar^c, J. Annaraj^a

^a Department of Materials Science, School of Chemistry, Madurai Kamaraj University, Madurai 21, India

^b Department of Chemistry, Pasumpon Muthuramalinga Thevar College, Usilampatti, Madurai 32, India[†]

^c Department of Physical Chemistry, School of Chemistry, Madurai Kamaraj University, Madurai 21, India

Received 6 August 2020; accepted 5 November 2020

Available online 16 November 2020

KEYWORDS

Dual chemosensor;
Para-magnetic metal couple;
Specific absorbance;
Molecular logic circuit and
in-vivo bio-imaging

Abstract Feasibly synthesized novel rhodamine based chemosensor (RS) has been described for the detection of paramagnetic and biologically important Cu²⁺ and Fe³⁺ ions. Among all the transition metal ions, this chemosensor was able to precisely spot out the Cu²⁺/Fe³⁺ ion couple by its spirolactam cleavage, consequently enhancing their absorbances at 521 and 529 nm for Cu²⁺ and Fe³⁺ ions respectively even at low concentrations [263 pM (Cu²⁺) and 2 nM (Fe³⁺)], which is prominently lower than the WHO and the United States Environmental Protection Agency (USEPA) strategies. This metal pair (Cu²⁺/Fe³⁺) has more tendencies to cleave the lactam ring even in the presence of higher concentrations of other relevant metal ions. Such remarkable behaviour of RS has been motivated us to apply zebrafish bio-imaging and molecular logic circuits.

© 2020 Published by Elsevier B.V. on behalf of King Saud University. This is an open access article under the CC BY-NC-ND license (<http://creativecommons.org/licenses/by-nc-nd/4.0/>).

1. Introduction

In the current world, the synthesis of fluorescent organic compounds has gained the utmost attention of researchers due to its widespread applications in various fields such as organic

light-emitting diodes fluorescent chemosensor, mechanosensors, bio-marker, and bioimaging (Yang et al., 2017; Li et al., 2017, 2018; Wang et al., 2017). Further the development and design of chemosensor to measure the metal ions in various real samples and living systems, in particular, have a vital significance due to the prominence of metal ions in the biological system and due to merits such as naked-eye detection, high selectivity, and more sensitivity (Gabr and Pigge, 2017; Sivaraman et al., 2012, 2018). Among the various transition metal ions special attention has always been dedicated to Cu²⁺ and Fe³⁺ metal ions due to, Among the various transition metal ions, special attention has always been dedicated to Cu²⁺ and Fe³⁺ metal ions due to their vital role as the active

[†] Affiliated to Madurai Kamaraj University, Madurai 21, India.

E-mail address: annaraj.chem@mkuniversity.org (J. Annaraj)

Peer review under responsibility of King Saud University.



catalytic centre in proteins/enzymes (Bensasson, 1997; Bannister, 1991) and plays important role in cell energy production. Moreover, such copper enzymes are involved in the activities of brain, liver, and kidney the cellular inadequacy of (Cu^{2+}) may lead to produce various acute diseases (Barnham et al., 2004; Davies et al., 2016; McDonald et al., 2014; Brown and Kozlowski, 2004; Xiao et al., 2013; Waggoner et al., 1999; Tang et al., 2020). Therefore the development of chemosensor to detect even a tiny level of Cu^{2+} ions in the biological system has garnered more attention in recent years. According to the United States Environmental Protection Agency (USEPA), the permitted maximum contamination level of Cu^{2+} and Fe^{3+} ions in drinking water is 1.3 ppm and $4.5 \mu\text{M L}^{-1}$ respectively (Kumar et al., 2015; Li et al., 2016) and the permissible level of copper in drinking water is $31.5 \mu\text{M}$ (Nayak et al., 2018).

Iron is a more critical metal ion and it can act as a reactive centre in enormous metalloenzymes such as haemoglobin, cytochromes, etc., and also acts as a catalyst in oxidoreductase reactions (Pithadia and Lim, 2012; Weizman et al., 1996; Bonda et al., 2011), and it is very essential to induce several cellular metabolism and synthesis of RNA and DNA (Burdo and Connor, 2003; Yin et al., 2011; Huang et al., 2012). Its deficiency in blood causes serious anaemia, while its excess may be associated with certain cancers and dysfunction of liver, heart, and nervous system (Kozlowski et al., 2009; Crichton et al., 2008). Additionally, its excess in living cell can damage the lipids, protein, and nucleic acids, etc., which leads the researchers to develop simple method for the determination of Fe^{3+} ions.

The existing methodologies for the determination of Cu^{2+} and Fe^{3+} ions includes, inductively coupled plasma mass spectrometry (ICP-MS), fluorescence, atomic absorption, colorimetry, flow injection, and electrochemical methods (Laglera and Monticelli, 2017; Zhao et al., 2018; Spolaor et al., 2012; Omarova et al., 2018; Qi et al., 2017). Compared to all the aforementioned methods, the fluorescence method has many advantages such as simplicity in handling, high selectivity, sensitivity, low cost, less time consuming, and minimum sample requirement for analysis (Liu et al., 2020; Zhu et al., 2017). Although, various fluorescent chemosensors have been reported as turn-off detectors towards $\text{Cu}^{2+}/\text{Fe}^{3+}$ ions (Zhao et al., 2009; Yang et al., 2012, 2016; Sikdar et al., 2012; Fatma et al., 2020), nevertheless, dye-based chemosensor have been utilized for the same. Among the reported dyes, rhodamine based chemosensor has considerable attention due to its photo-physical and good bio-compatibility properties (Deng and Xu, 2019). In addition, its spiro-lactam ring can be easily opened in the presence of acids consequently leading to an excellent fluorescence. This ignites the researchers to develop novel chemosensors for the recognition of biologically and environmentally important metal ions, since the chemosensors based on rhodamine may be utilized as labelling agent for the heavy metal ions such as Cu^{2+} , Hg^{2+} , Pb^{2+} , and Fe^{3+} ions (Cheng et al., 2014; Li et al., 2016; Fang et al., 2015; Cherreddy et al., 2012; Kwon et al., 2005).

Generally, fluorescent sensors are focused on identifying the distinct analyte selectively, while recently researchers have shown much interest towards dual or multi-ion chemosensor, especially for Cu^{2+} and Fe^{2+} . Simple sensors could be able to trace the environmentally and biologically significant multiple target ions are highly proficient, cost-effective and easy to

handle (Fatma et al., 2020). In the last few decades, there are a significant number of cation-cation or cation-anion or anion-anion dual sensors reported (Cheng et al., 2014; Li et al., 2016; Patra et al., 2016; Singh et al., 2015). Among them, detecting a pair of paramagnetic metal ions ($\text{Fe}^{3+}/\text{Cu}^{2+}$) is very scanty and those probes have disadvantages such as poor selectivity, difficulties in distinguishing those paramagnetic metal ions and interference of some metal ions during experiments (Choi et al., 2014; Yang et al., 2016). Here we report an innovative fluorescence chemosensor which is constructed with rhodamine 6G and dihalo substituted salicylaldehyde (RS) and it can be successfully applied to the molecular logic gate and in-vivo bio-imaging studies. To the best of our knowledge, this is the first report for the detection of $\text{Fe}^{3+}/\text{Cu}^{2+}$ ion pair in two different wavelengths by a single probe using absorbance spectroscopy.

2. Experimental section

2.1. Materials and methods

All the solvents and reagents (analytical and spectroscopic grade) were obtained from Sigma-Aldrich and used without further purification. Metal chloride and nitrate salts were purchased from Merck and used as such. NMR spectra were recorded using Bucker 300 MHz spectrophotometer. The chemical shifts were shown in parts per million (ppm) downfield from tetramethylsilane (reference chemical shift is zero ppm) using residual DMSO (internal standard). Multiplicities were reported as follows: s (singlet), d (doublet), t (triplet), m (multiplet), and br (broadened). All the absorption measurements were recorded using Jasco 630 spectrophotometer and fluorescence measurements were performed in Agilent Cary Eclipse fluorescence spectrophotometer at room temperature. Electrospray ionization mass spectra (ESI-MS) were collected on liquid chromatography-ion trap mass spectrometer at room temperature (LCQ Fleet, Thermo Fisher instruments limited, USA).

2.2. UV-visible and fluorescence titrations

An acetonitrile solution of RS ($2.5 \mu\text{M}$) has been used for the absorption and fluorometric spectral titrations. Slit width of 5/5 and 375 nm as an excited wavelength for all fluorescent measurements. Freshly prepared probe solution has been used in each experiment, and the corresponding metal ions were added using micropipette. The UV-visible and fluorescence spectral experiments were performed with high concentration of chemosensor RS (10^{-3}M) in DMSO as a stock solution to avoid the dilution error. 10 equivalents of all the biologically important metal ions were used for the selectivity experiment with respect to the probe and $\mu\text{M}/10^{-7}\text{M}$ of $\text{Fe}^{3+}/\text{Cu}^{2+}$ ions were used for the sensitivity experiments respectively. In the jobs plot analysis, $10 \mu\text{M}$ of analyte and chemosensor RS were used respectively in both spectroscopic techniques.

2.3. Fluorescence imaging on embryos

Three days old embryos were pre-treated with Fe^{3+} ions for 2 h, and washed with phosphate buffer. These iron pre-treated embryos were treated with $2.5 \mu\text{M}$ of RS solution for

1 h and they were again washed with phosphate buffer solution. Finally, these were fixed in 10% methylcellulose solution for secured orientation and then fluorescent images were recorded by fluorescence microscopy.

2.4. pH studies

The medium adopted to proceed the experiments under varying pH gradients have been carried out using 0.1 M of hydrochloric acid and triethylamine to adjust the pH. The individual pH solution of acetonitrile has been prepared in the range of 2–12. Before recording the absorbance and fluorescence spectra, the invivual pH of the chemosensor, RS and $\text{Cu}^{2+}/\text{Fe}^{3+}$ ion solutions were examined to the respective pH gradient at room temperature.

3. Results and discussion

3.1. Synthesis of chemosensor, RS

Rhodamine hydrazine was synthesised by the previously reported procedure (Ma et al., 2013) with slight modifications. Rhodamine 6G (1 mmol) and hydrazine monohydrate (5 mmol) was dissolved in methanol and this reaction mixture was refluxed for 2 h, a pinkish white precipitate was obtained, which was filtered and washed with cold methanol then dried at room temperature. This rhodamine hydrazide was re-dissolved in hot methanol and 1 equivalent of 3,5-diiodo salicylaldehyde is added to it and refluxed for 3 h, it was cooled to room temperature yielding the desired chemosensor RS, as pale yellow solid which was filtered and washed with cold methanol (yield 72%) (Scheme 1). It was characterized by NMR and ESI-MS analysis. ^1H NMR (300 MHz, DMSO) δ 11.87 (s, 1H), 8.68 (s, 1H), 7.95 (d, $J = 6.3$ Hz, 2H), 7.77–7.49 (m, 3H), 7.06 (d, $J = 7.1$ Hz, 1H), 6.35 (s, 2H), 6.20 (s, 2H), 5.16 (t, $J = 5.2$ Hz, 2H), 3.23–3.03 (m, 4H), 1.84 (s, 6H), 1.20 (t, $J = 7.1$ Hz, 6H) (Fig. S1). ^{13}C NMR (75 MHz, DMSO) δ 164.62, 157.04, 152.35, 151.91, 148.94, 148.78, 147.73, 139.75, 135.24, 129.80, 128.53, 127.56, 124.68, 124.13, 121.25, 119.49, 104.62, 96.85, 88.52, 82.82, 66.64, 41.38, 41.10, 40.82, 40.54, 40.26, 39.98, 39.71, 38.36, 17.71, 15.01

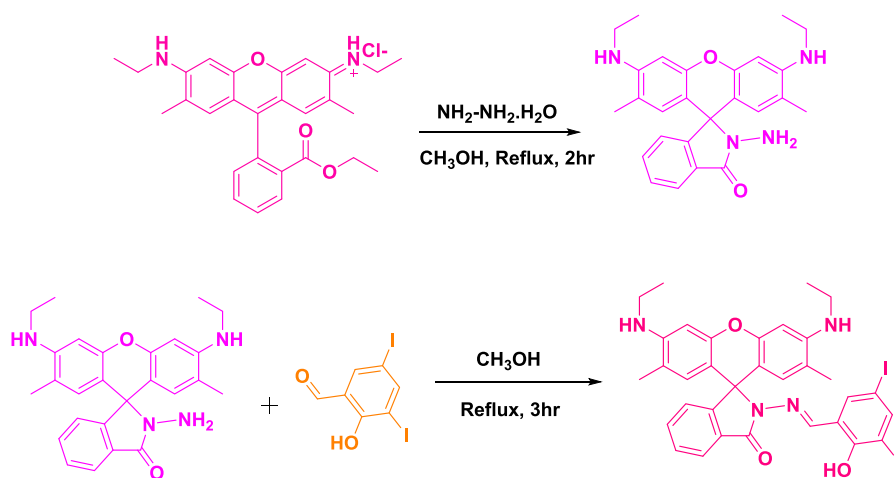
(Fig. S2). Calculate Mass = 784.04. Mass obtained from ESI-MS: $m/z = 785.05$ ($M + 1$) (Fig. S3). Obtain mass from HR-MS: 785.0434 ($M + 1$) (Fig. S4).

3.2. Naked eye and fluorescence sensor

A stock solution was prepared with the synthesised chemosensor RS (3.9 mg) in DMSO (5 mL). This stock solution has been diluted to 2 mL in acetonitrile and cover up concentration of 2.5 μM , which was used for all sensor studies. To evaluate its naked eye sensor abilities, 10 equivalents of various biologically and environmentally important metal ions have been used (Fe^{3+} , Fe^{2+} , Cu^{2+} , Al^{3+} , Cr^{3+} , Pb^{2+} , Cd^{2+} , Hg^{2+} , Zn^{2+} , Ni^{2+} , Co^{2+} , Mn^{2+} , Mg^{2+} , Ba^{2+} and Ca^{2+}). The non-fluorescent RS did not show any significant fluorescence changes upon the addition aforementioned metal ions with the exception of Fe^{3+} and Fe^{2+} ions. The addition of Fe^{3+} ions leads to an intense fluorescence change in the UV cabinet along with a puny fluorescence due to Fe^{2+} ions, because of the Lewis acidic nature of Fe^{3+} ions, and its tendency to cleave the lactam ring present in the RS. Interestingly, the occurred colour changes of RS with Fe^{3+} (pale pink) and Cu^{2+} (intense pink) ions in CH_3CN could also be monitored by the naked eye. These observed colorimetric and fluorescence sensing studies could indicate that the probe can be efficiently utilized for the selective detection of $\text{Fe}^{3+}/\text{Cu}^{2+}$ ions (Fig. 1).

3.3. Fluorescence studies

Generally, acids (organic/inorganic) can be used to stimulate and open the existing locked lactam ring in the chemosensor RS, which could enhance the fluorescence/absorbance (Bao et al., 2019; Karakus et al., 2013; Queirós et al., 2014). As like, inorganic Lewis acid, Fe^{3+} ions can also trigger the opening of the existing lactam ring in the proposed probe RS, which leads to excellent photo-physical properties at 554 nm. On the addition of 10 equivalents of various biologically important metal ions didn't show any new band in a emission profile except Fe^{3+} ions, shows a bright fluorescence at 554 nm (Fig. 2a). Similarly, the existing unpaired electron in Fe^{2+} ion, it also



Scheme 1 Chemical synthesis of the chemosensor RS.



Fig. 1 Photograph of chemosensor, RS (2.5 μM) with various metal ions in (a) normal day light (RS, Fe^{3+} , Fe^{2+} , Cu^{2+} , Al^{3+} , Cr^{3+} , Pb^{2+} , Cd^{2+} , Hg^{2+} , Zn^{2+} , Ni^{2+} , Co^{2+} , Mn^{2+} , Mg^{2+} , Ba^{2+} and Ca^{2+} left to right) and (b) fluorescence lamp (RS, Fe^{3+} , Fe^{2+} , Cu^{2+} , Al^{3+} , Cr^{3+} , Pb^{2+} , Cd^{2+} , Hg^{2+} , Zn^{2+} , Ni^{2+} , Co^{2+} , Mn^{2+} , Mg^{2+} , Ba^{2+} and Ca^{2+} left to right).

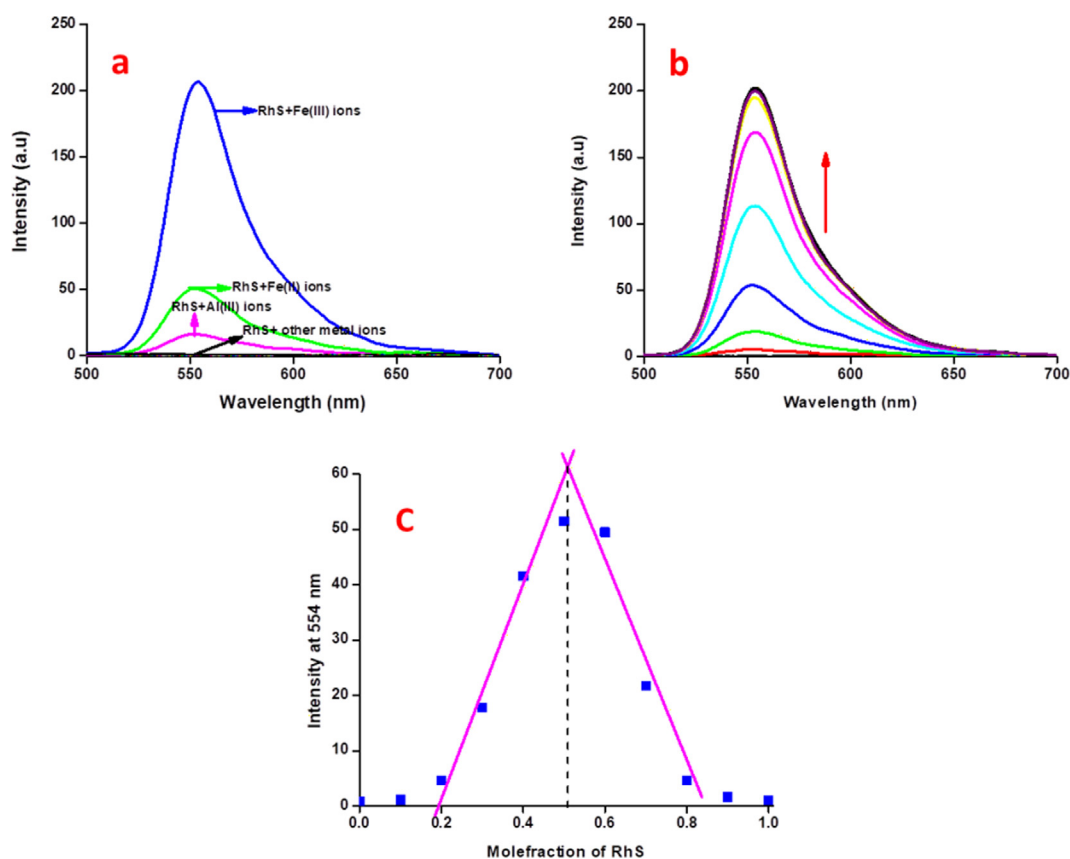


Fig. 2 (a) Fluorescence selectivity spectral analysis of RS (2.5 μM) with 10 equivalents of other relevant metal ions in $\text{CH}_3\text{CN}:\text{H}_2\text{O}$ (9:1 v/v) mixture, (b) Fluorescence sensitivity spectral analysis of RS (2.5 μM) with incremental addition of Fe^{3+} ions (0–22.5 μM) in $\text{CH}_3\text{CN}:\text{H}_2\text{O}$ (9:1 v/v) mixture, (c) Job's plot analysis of Fe^{3+} ions with respect to the mole-fraction of RS at 554 nm in fluorescence spectroscopy.

showed a trivial fluorescence enhancement over the Fe^{3+} ions. In order to check out the sensing propensity of RS analysis between static concentration of RS and increasing concentrations (0–22.5 μM) of Fe^{3+} ions was performed (Fig. 2b). The incremental addition of the Fe^{3+} ions yields a gradual appearance of a new band at 554 nm with clear linearity (7.5–17.5 μM , Fig. S5), further addition of excess Fe^{3+} ions leads to saturation. These studies demonstrated that the chemosensor RS tends to recognize Fe^{3+} ions quantitatively. Such accurate quantity of limit of detection (2 nM) could be

calculated by using the formulae $3\sigma/\text{slope}$. Chemosensor RS has also showed a strong binding constant ($3.4 \times 10^{-1} \text{M}^{-1}$, Fig. S6) with Fe^{3+} ions. The stoichiometry of RS- Fe^{3+} complex was determined using Job's method by the plot between the intensity of conjugate, RS- Fe^{3+} with respect to the mole-fraction of RS, which clearly exposed that its efficient and intense fluorescence band was observed at 0.5 mol-fraction. This observation indicated that the occurrence of 1:1 mode of binding between RS and Fe^{3+} ions (Fig. 2c). Further ahead, RS showed a good sensing knack towards Fe^{3+} ions even in

the presence of high concentrations of the other metal ions except Cu^{2+} ions, which may be due to the Cu^{2+} scavenging on the excited-state electron from RS-Fe^{3+} complex. Moreover, the addition of Fe^{2+} ions also causes a small interference in the fluorescence of RS-Fe^{3+} conjugate.

3.4. Absorption spectroscopy

Chemosensor RS showed two absorption bands at 300 and 350 nm. These bands are attributed to its $\pi\text{-}\pi^*$ and $n\text{-}\pi^*$ transitions, and there is no absorbance was appeared in the range of 500–600 nm. Interestingly, addition of 10 equivalents of Cu^{2+} and Fe^{3+} ions, showed an excellent chromo-isomerism with rigid absorption bands at 521 and 529 nm respectively as a consequence of the cleaved spirolactam ring (Lewis acidic nature of these two paramagnetic metal ions) exist in the RS, while, other metal ions did not show any significant colour or spectral changes (Fig. 3a).

The cation-sensing mechanism of RS is based on the change in its structure between spirocyclic locked-form to ring-opened form due to the chelation and lewis acidity of metal ions, which leads to the appearance of intense pink colour as shown in Scheme 2. The chemosensor RS is colourless and non-fluorescent in aqueous CH_3CN solution. While, upon addition of Cu^{2+} , leads its chelation with chemosensor RS may simultaneously open the spirolactam ring and convert the RS into its ring-opened form along with a remarkable colour change

of experimental solution. Such changes enhanced the electronic absorption responses at 521 nm performed as substantial colorimetrically off/on sensing probe. Hence, the addition of Fe^{3+} ions enhanced the chemosensor RS absorbance at 300 and 350 nm, but such spectral changes were lacking in the presence of Cu^{2+} ions. Instead, decrement of RS absorbance along with a rigid band was observed at 401 nm due to ligand to metal charge transfer.

These dissimilar observations of Cu^{2+} and Fe^{3+} ions may due to their lewis acidic nature and chelation effect. Even though Cu^{2+} ions are paramagnetic in nature, it is highly unstable consequently more reactive may due to its d^9 system, while Fe^{3+} ions have five unpaired electrons and highly stable due to its half-filled d^5 electronic state. Hence, Fe^{3+} ion has more lewis nature than the Cu^{2+} ions, moreover, Cu^{2+} ion has a great tendency to involved in chelation with ligand/probe than Fe^{3+} ions. Therefore, Fe^{3+} ions could be able to open the spiro-lactam ring very quickly, later it interacts with the donor site of the chemosensor RS formed week complex, instead Cu^{2+} ions are rapidly involved in chelation leads to complexation, simultaneously this complex may lead to open the lactam ring. Due to this rapid formation of chelation with chemosensor RS, the absorption bands at 300 and 350 nm responsible for RS underwent decrement in its intensity, and appearance of new band at 401 nm may occurred due to Ligand to Metal Charge Transfer (LMCT).

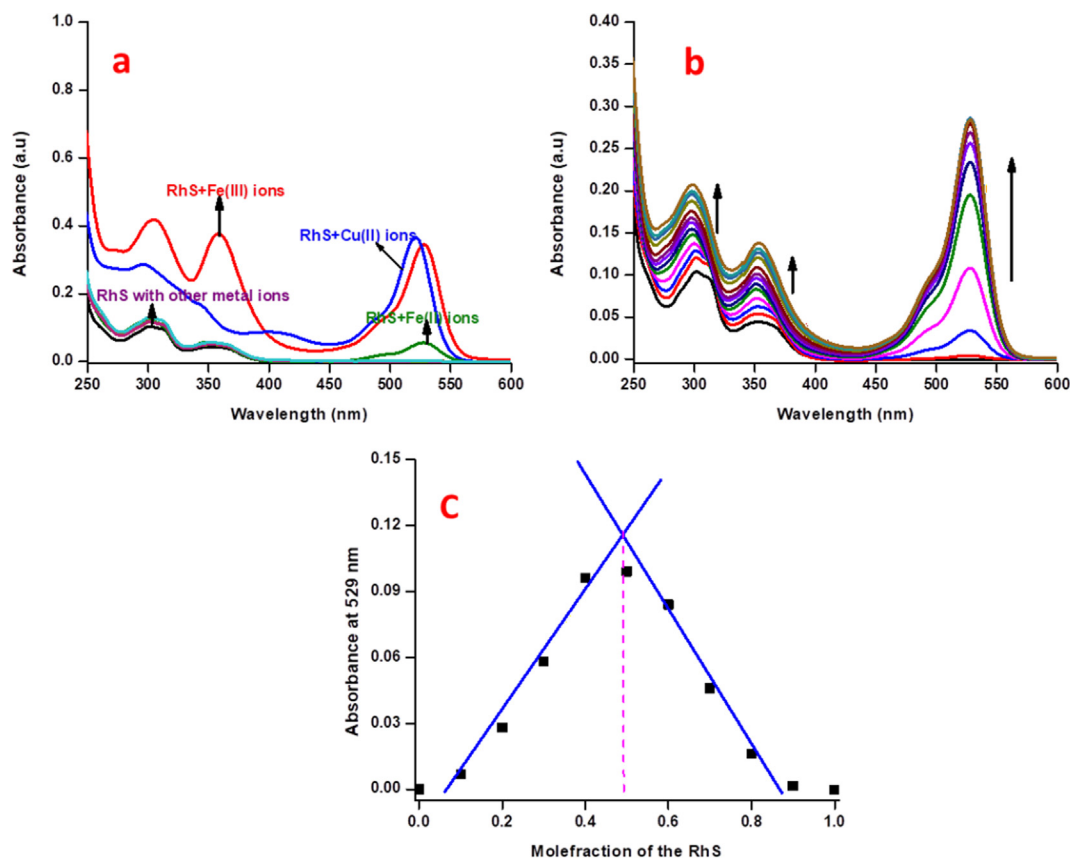
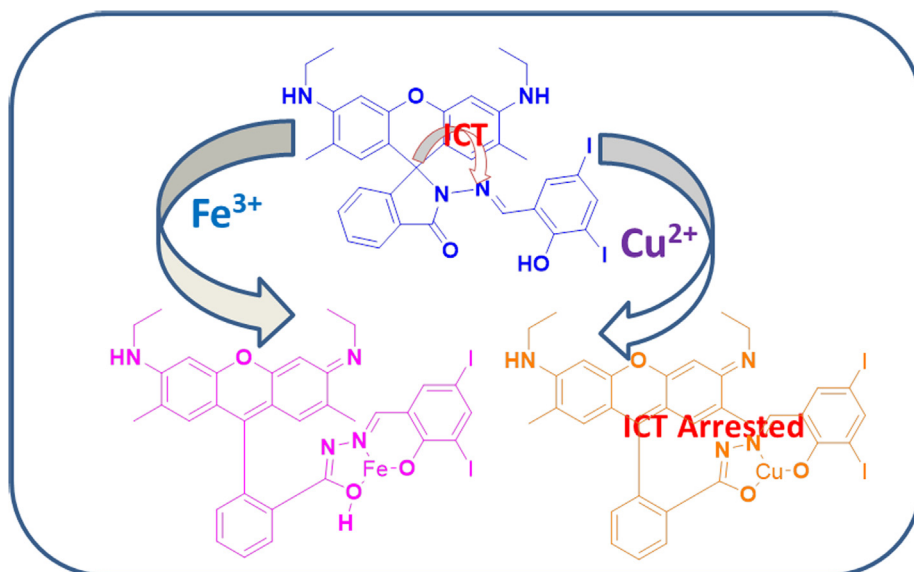


Fig. 3 (a) Electronic absorbance selectivity spectra of RS (2.5 μM) with 10 equivalents of other relevant metal ions in $\text{CH}_3\text{CN}:\text{H}_2\text{O}$ (9:1 v/v) mixture, (b) absorption spectral sensitivity analysis of RS (2.5 μM) with incremental additions of the Fe^{3+} ions in $\text{CH}_3\text{CN}:\text{H}_2\text{O}$ (9:1 v/v) mixture, (c) Job's plot analysis of Fe^{3+} ions with respect to mole-fraction of the RS in absorbance spectroscopy.



Scheme 2 Proposed sensing mechanism of the chemosensor RS and its $\text{Cu}^{2+}/\text{Fe}^{3+}$ complexes.

Sensitivity titrations were performed to find out the sensing ability of RS towards Fe^{3+} ions. Upon the incremental additions of Fe^{3+} ions (0–30 μM) to RS solution a gradual generation of a new band at 529 nm and linear absorption enhancements at 300 and 350 nm along with a small blue shift were observed (Fig. 3b) until the concentration range of 5–12.5 μM (Fig. S7). Further addition of Fe^{3+} ions leads to their saturation, indicating that the locked spiro-lactam has been opened which is reliable with that of fluorescence spectra, and demonstrating RS can aid as a “naked-eye” chemosensor for Fe^{3+} ions in aqueous CH_3CN solution. In addition, the detection limit for Fe^{3+} ions was found to be 3.1 nM with a binding constant of $5.2 \times 10^{-2} \text{ M}^{-1}$, which was determined by B-H equation (Fig. S8). The stoichiometry between RS and Fe^{3+} ions were determined by Jobs plot method, it clearly indicates that the probe will interact with Fe^{3+} ions in 1:1 binding fashion (Fig. 3c).

The addition of Cu^{2+} ions with RS solution, a gradual appearance of band at 521 nm along with three enhancements at 332, 270, and 401 nm was observed. In addition, gradual decrease in absorbance at 300 and 350 nm were also observed along with four isosbestic points at 374, 351, 321, and 290 nm,

which leads to a visible colour change from colourless RS to intense pink which may be due to the attained equilibrium between free copper ions and in-situ formed RS-Cu complex at corresponding wavelengths (Fig. 4a). Such spectral changes were not observed for Fe^{3+} ions, due to its spiro-lactam ring opening behaviour rather than stable complex formation as like RS- Cu^{2+} . Sensitivity experiment showed a good linear relationship up to the concentration of $55 \times 10^{-7} \text{ M}$ (Fig. S9) which was used to find out the lowest detection limit in aqueous CH_3CN (1:1, v/v) of 263 pM and binding constant of $1.1 \times 10^{-2} \text{ M}^{-1}$ (Fig. S10). Job's plot has exposed a maximum absorbance at 521 nm with 0.5 mol fraction of the RS (Fig. 4b). The stoichiometry of the Fe^{3+} and Cu^{2+} ions has been confirmed by the ESI-MS spectrometer. It shows that the m/z value of 863.6 ($\text{M} + \text{Na}$) and 847.10 ($\text{M} + 1$) for Fe^{3+} and Cu^{2+} ions respectively (Fig. S11,S12).

3.5. Interference experiment

The competitive experiments have been carried out between 10 equivalents of $\text{Cu}^{2+}/\text{Fe}^{3+}$ ions and 15 equivalents of other rel-

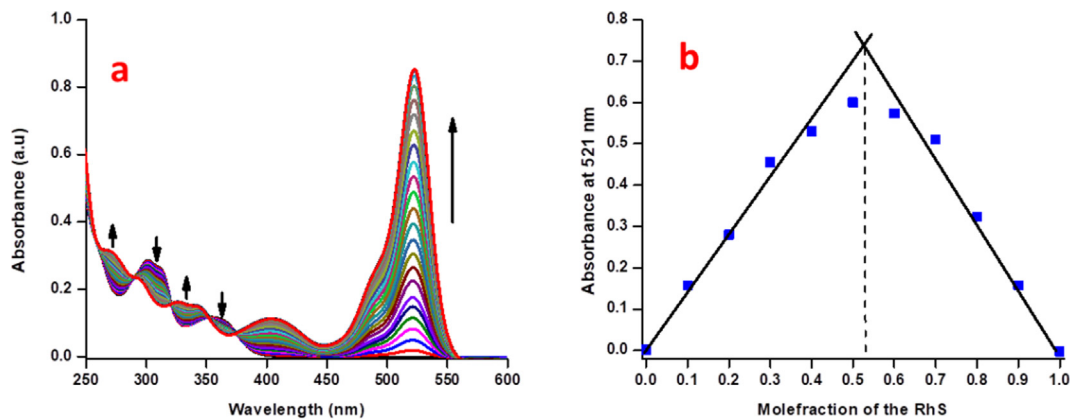


Fig. 4 (a) Absorption spectral sensitivity analysis of RS (2.5 μM) with incremental additions of the Cu^{2+} ions in $\text{CH}_3\text{CN}:\text{H}_2\text{O}$ (9:1 v/v) mixture, (b) Job's plot analysis of Cu^{2+} ions with respect to mole-fraction of RS in absorbance spectroscopy.

evant metal ions towards RS. The observed results showed that the chemosensor RS could be able to selectively recognize $\text{Fe}^{3+}/\text{Cu}^{2+}$ ion couple rather than other metal ions (Fig. 5a and b). The competition between Cu^{2+} and Fe^{3+} ions towards RS was also analysed using electronic absorption and fluorescence spectroscopic techniques. In the presence of both $\text{Fe}^{3+}/\text{Cu}^{2+}$ metal ions, chemosensor has expressed its great tendency of attraction towards Fe^{3+} ions than Cu^{2+} ions, due to the quick spectrolactam ring cleavage existing in RS by Fe^{3+} ions which leads to more resonance of xanthyl moiety rather than the stable chelation of Cu^{2+} ions, which is also agreed with the aforementioned greater binding constant value of Fe^{3+} ions than Cu^{2+} ions. The observed fluorescence spectral changes showed only partial quenching during the addition of Cu^{2+} ions, while absorbance was enhanced, which may be due to scavenging of the excited state electron of iron complex by copper ions (Fig. 5c). This crucial process can only be detected in fluorescence spectroscopy due to its higher sensitivity, while not in the absorbance spectroscopy. This partial quenching effect could be reduced by the addition of cysteine. Upon addition of cysteine, leads the formation of cysteine copper complex initially (Yang et al., 2019; Lee et al., 2015; Senthil Murugan et al., 2020) and it creates free environment around Cu^{2+} ions, it causes for a significant enhancement in the fluorescence of iron complex (Fig. S13). Moreover, this competitive experiment has also been done in ESI-MS spectroscopy. The obtained m/z value of 845.4 and 863.9 which is attributed to the Cu^{2+} and Fe^{3+} complexes respectively and the peak for

the copper complex has less intensity than the iron complex, these observations concluded that the chemosensor has more affinity towards Fe^{3+} than the Cu^{2+} ions (Fig. S14).

3.6. NMR studies

NMR spectroscopy is also used to understand the binding nature of metal ions with chemosensor RS. For the NMR studies, 8 mg of the RS in 0.4 mL of deuterated DMSO was treated with one equivalent of each metal ion ($\text{Fe}^{3+}/\text{Cu}^{2+}$) individually in 0.1 mL of deuterated water. First, we performed RS alone and then metal ions were added to the RS solution in individual NMR tubes and shaken well before the each experiment. The chemosensor RS showed two singlet peaks at deshield region which is attributed to phenolic $-\text{OH}$ of salicylaldehyde (11.87 ppm) and azomethine (8.68 ppm) proton of imine bond (Fig. 6a). The addition of one equivalent Cu^{2+} ions on RS, its existing peak at 11.87 ppm was utterly vanished along with shielded imine peak (8.65 ppm) were observed (Fig. 6b). On the other hand, addition of one equivalent Fe^{3+} ion, the peak at 11.87 ppm became broaden with a decrement in its intensity and a slight deshielding (11.90 ppm) as observed. This study obviously indicates that the Cu^{2+} ions are involved in deprotonation of phenolic $-\text{OH}$ due to its strong chelation through oxygen and imine nitrogen atoms present in the chemosensor. While addition of Fe^{3+} ions, does not deprotonate its phenolic $-\text{OH}$, however it interacts strongly

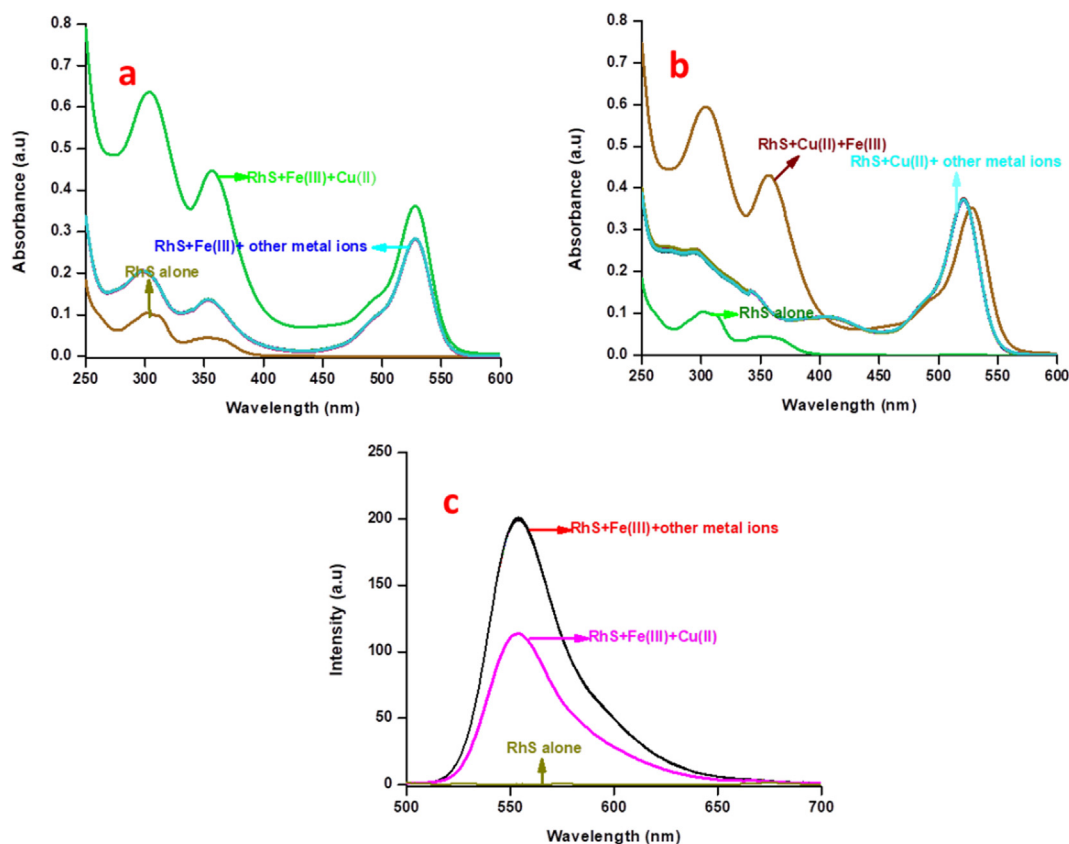


Fig. 5 Absorption spectral interference analysis of RS with 10 equivalents of Fe^{3+} in the presence of 15 equivalents of other metal ions, (b) Absorption spectral interference analysis of RS with 10 equivalents of Cu^{2+} in the presence of 15 equivalents of other metal ions, (c) Fluorescence spectral interference analysis of RS with 10 equivalents of Fe^{3+} in the presence of 15 equivalents of other metal ions.

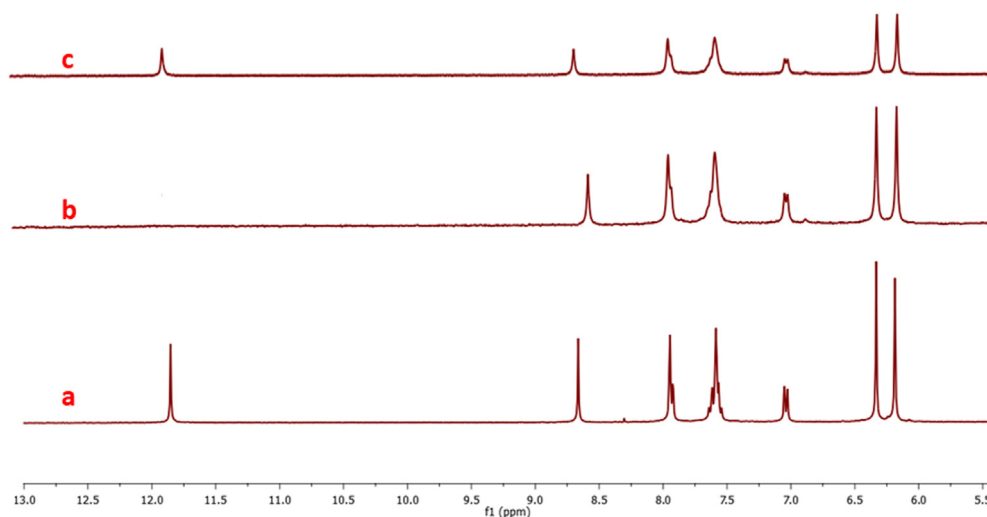


Fig. 6 ^1H -NMR spectra of the probe RS (a) with one equivalent of copper ions (b) one equivalent of copper ions and (c) one equivalent of iron ions.

with imine peak leads to deshielding which means the double bond character of the $\text{C}=\text{N}$ has reduced, as a consequence the spiro-lactam ring has been opened (Fig. 6c). These studies clearly show that the metal ions are involved in typical chelation interaction rather than acid hydrolysis.

3.7. Theoretical studies

To comprehend the ICT mechanism underlying the experimentally observed photophysical properties of RS upon its spiro-lactam ring open due to Fe^{3+} and chelation with Cu^{2+} , we had explored the structural, electronic, and optical properties using Gaussian 09 package. Here we have derived HOMO, LUMO, and LUMO + 1 of the chemosensor RS and its complexes ($\text{Cu}^{2+}/\text{Fe}^{3+}$) as shown in Fig. 7. The energy difference between the HOMO and LUMO/LUMO + 1 for RS are 3.69 and 3.73 eV respectively. This energy gap has been significantly quenched by complex formation with $\text{Cu}^{2+}/\text{Fe}^{3+}$ ions. The Cu^{2+} -RS complex showed 2.43 eV for HOMO-LUMO and 2.84 eV for HOMO-LUMO + 1, while the Fe^{3+} -RS has shown 1.35 eV for HOMO-LUMO and 2.40 eV for HOMO-LUMO + 1. Such energy difference clearly confirms the occurred strong interaction between RS and $\text{Fe}^{3+}/\text{Cu}^{2+}$ cations. The existing xanthyl moiety in RS acts as HOMO, and the electrons were distributed over the whole Schiff's base moiety at LUMO and LUMO + 1. It illustrated that the chemosensor has an intra charge transfer process while the lactam ring is closed. Cu^{2+} -RS complex has more electron cloud on the copper centre in HOMO, indicating that the copper ions are strongly bound with RS at the ground state level. Since the spiro-lactam ring has opened during the course of addition of Fe^{3+} ions, the electrons were moved towards the xanthyl moiety at LUMO leads to appear as strong pink colour, which could be observed even by the naked eye. This obtained HOMO-LUMO energy difference in DFT calculation was observed at 510 nm, which is closely agreed to the early obtained absorbance (521 nm) of RS by the addition of Cu^{2+} ions in the electronic spectroscopic studies.

More interestingly, RS-Fe complex showed a very low energy difference between HOMO and LUMO than RS-Cu

complex, which may be due to the formation of excited state RS-Fe complex like LUMO + 1 rather than at ground state, as a consequence a significant enhancement was observed in the fluorescence. RS-Fe complex also has electron densities on xanthyl moiety at HOMO, and on Schiff's base portion at LUMO and LUMO + 1, respectively. However, the electron transition may occur from HOMO to LUMO + 1 at 516 nm and is practically firm the absorbance (529 nm) observed in the UV-vis spectroscopy. Here, the existing dihalo substituted salicylaldehyde group in this chemosensor RS is having the electron deficiency on the Schiff base moiety. Due to this, the imine nitrogen carries a slightly positive charge and it has pulled the electron from the xanthyl moiety. Thus, Schiff base part acts as an acceptor and xanthyl moiety as a donor site. Based on the aforementioned observation, the chemosensor RS showed a clear ICT from xanthyl group to Schiff's base moiety, while this ICT process has been arrested in the presence of copper ions due to Cu^{2+} ions are involved in strong chelation at the ground state so that imine nitrogen has provided electron to the Cu^{2+} ions and its plugged in the whole electron towards itself. This happened only at the ground state HOMO level whereas the excited state has more electron density on the xanthyl moiety because the Cu^{2+} ions only interact at ground state and are not disturbing the excited state electron distribution. In addition, its counterpart (iron complex, RS-Fe) has a very low energy gap between HOMO and LUMO (than the RS and its copper complex), illustrated that the Fe^{3+} ions induced the fluorescence of the xanthyl group rather than the formation of ground state complex. Based on theoretical and spectral studies, the mechanism has been proposed in Scheme 2.

3.8. Reversibility and stability

Reversibility is one of the significant criteria for chemosensor. Henceforth, we performed reversibility experiments between RS and EDTA, and it showed good reversibility with EDTA complexes up to five cycles. As we mentioned earlier, the colourless RS did not show any absorbance in the range of 500–600 nm, while the addition of $\text{Cu}^{2+}/\text{Fe}^{3+}$ ions generates

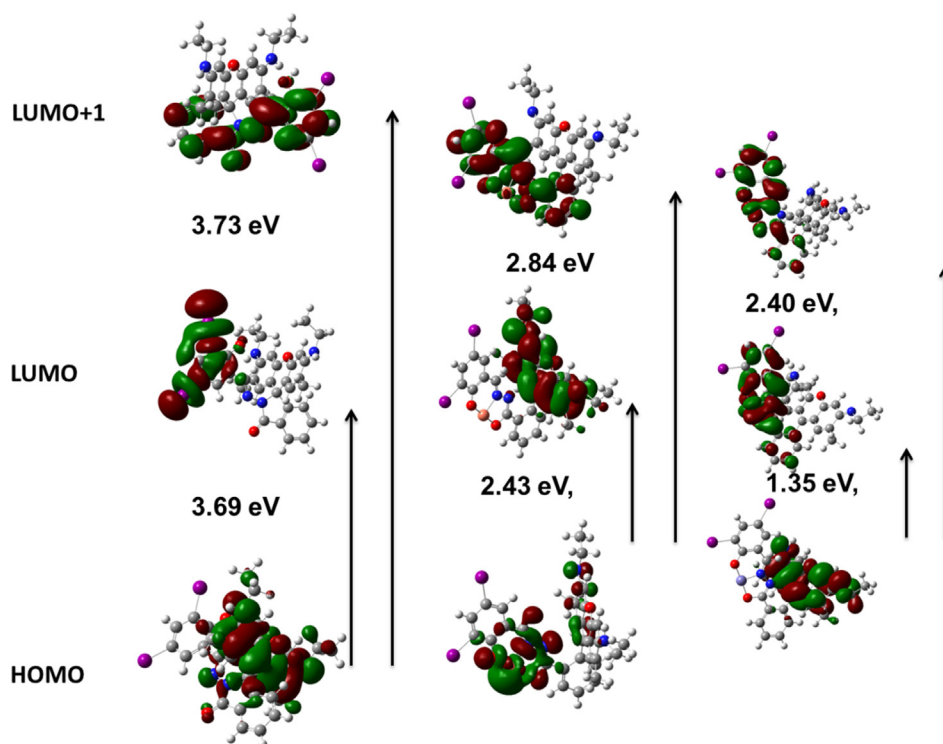


Fig. 7 DFT analysis of the chemosensor RS, RS-Cu and RS-Fe (left to right).

new peaks at their respective characteristic wavelengths. The subsequent additions of EDTA leads to de-metalation of individual (Cu^{2+} -RS and Fe^{3+} -RS) complexes and retained the absorbance and fluorescence of probe RS alone. These observations clearly indicate that RS could potentially be able to sense $\text{Fe}^{3+}/\text{Cu}^{2+}$ ions and also has tendency to reproduce RS by the addition of EDTA (Fig. S15-S17).

In general, the light-sensitive rhodamine in solution state, which exhibited excellent colour and fluorescent changes due to its spiro lactam ring induced to open by photons. Hence, it is also essential to find out the stability of RS in solution state. In order to carry out this, we prepared 10^{-3} M DMSO solution of RS as a stock solution and examined its stability by using absorbance spectroscopy. The required dilution has been done with this stock solution suitable for the present sensor system and recorded the absorbance spectra. Once every 3 days, we have monitored its absorbance and observed that the chemosensor has shown excellent stability for up to 30 days (Fig. S18).

3.9. pH studies

The absorbance and fluorescence spectra were recorded for RS and with $\text{Cu}^{2+}/\text{Fe}^{3+}$ metal ions at various pH (2–12) gradients. Fig. 8 shows that the probe has opened the ring at higher pH on higher absorbance and fluorescence. This may due to the protonation of lactam carbonyl group, which triggered the opening of the spiro lactam ring. The absorbance and fluorescence of the chemosensor RS were inactive at pH of greater than 5. This clearly notified that the spiro lactam ring has been induced to open only at acidic pH gradients of 2 to 4, it sustained its closed form at the higher pH (>5). On the other hand, the sensing of the Cu^{2+} and Fe^{3+} also performed at

the same pH range. Interestingly, RS is more active at the biological pH (5–7) with both metal ions. Moreover, Fe^{3+} ions lead to a small dwindle in both absorbance and fluorescence at higher pH (8–12) gradients, due to the possible interaction between trimethylamine (base) and Fe^{3+} ions, consequently the lewis acidic character of Fe^{3+} ions gets decrease.

3.10. Live cell imaging studies on zebra fish embryos

To investigate the applicability of this chemosensor RS with excellent sensing properties by fluorescence microscopic imaging studies were conducted by incubating Zebrafish embryos with Fe^{3+} ions. Since zebrafish embryos have thin skin which could easily convey its fluorescence, hence researchers mostly have chosen zebrafish embryos as a prominent animal model vertebrate for *in-vivo* live-cell imaging applications. In addition, recent reports reveal that these zebrafish embryos can be used as a model for various human diseases (Zon, 1999). Initially, the toxicity of the proposed chemosensor RS and Fe^{3+} ions on zebrafish embryos was examined for four days, and then the mortality rate of the zebrafish embryos was monitored. It exposed that the RS and Fe^{3+} ions showed very minor toxicity towards them (Fig. S19). This lower mortality result induced us to carry out the *in-vivo* imaging studies. There were two sets of embryos were treated with Fe^{3+} ions and chemosensor RS, then monitored under fluorescence microscopy. As we mentioned earlier, the non-fluorescent RS did not show any significant response in spectroscopic technique as well as in zebrafish embryos. Fig. 9a, b and c refers to bright, fluorescence and merge field images of the RS alone. While the embryos were pre-treated with Fe^{3+} ions exhibited an excellent yellow fluorescence with chemosensor RS. Fig. 9e clearly shows that most of the Fe^{3+} ions are

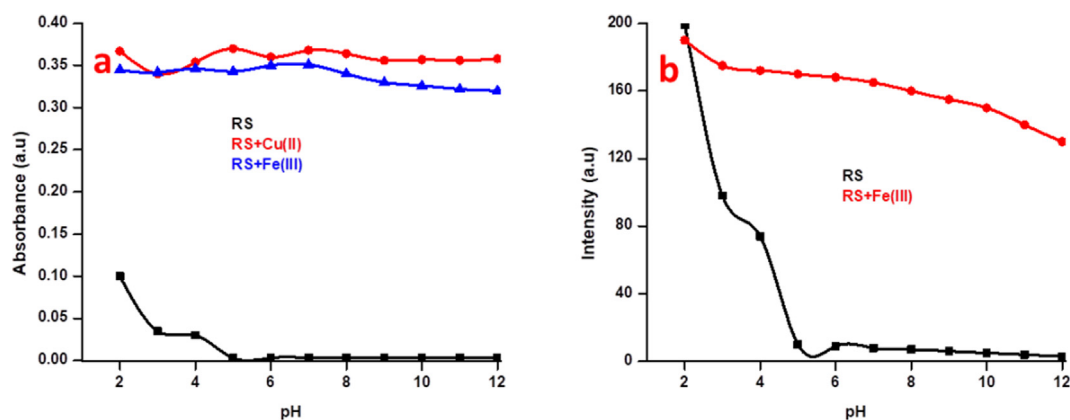


Fig. 8 (a) pH studies of RS (2.5 μM) with 10 equiv. of Cu^{2+} and Fe^{3+} ions in various pH solutions in absorbance spectroscopy and (b) pH studies of RS (5 μM) with 10 equiv. of Fe^{3+} ions in various pH solutions in fluorescence spectroscopy at excitation wavelength of 375 nm. the absorbance were taken at 521 and 529 nm for $\text{Cu}^{2+}/\text{Fe}^{3+}$ respectively and emission at 554 nm were taken for the fluorescence spectroscopy.

accumulated at the abdomen part of the embryos and exhibit a bright fluorescence with RS. These observed results exactly revealed that the RS could be efficiently utilized for the detection of the Fe^{3+} ions in biological species.

3.11. Molecular logic gates

Lately, researchers are infatuated to develop molecular logic gates by using the supra-molecular system. That will be achieved mainly with a system consisting of chemically encoded information as inputs and its emission or absorbance properties as output. As the previous observations illustrated

that this chemosensor RS could be able to recognize $\text{Fe}^{3+}/\text{Cu}^{2+}$ ions *via* two different analytical modes (UV-visible and fluorescence methods) with different wavelengths, it can also be utilized as a molecular-scale logic device. In the absence of chemical inputs ($\text{Fe}^{3+}/\text{Cu}^{2+}$), RS did not show any band in the range of 500–600 nm in electronic absorption and fluorescence spectral techniques. The addition of 1 equivalent of Cu^{2+} or Fe^{3+} ions generates new bands at 521 and 529 nm in the electronic absorption spectroscopy. Likewise, a new fluorescent band was also observed at 554 nm in the presence of Fe^{3+} ions. If it is active in the electronic absorption and fluorescence spectra, it is denoted as 1 and at the inactive stage, it is denoted as 0. In the same way, it is denoted as 1 in the presence of analytes and 0 in their absence. Based on the absorbance and emission spectroscopic observations, the truth table (Table 1) could be constructed and a new molecular logic circuit is developed, which exactly mimics the present sensor system (Fig. 10).

3.12. Comparison with recent reports

Since the existing few literature reports as dual sensors of two paramagnetic metals using different analytical tool, have several demerits such as sensitivity, limit of detection and having some interference with others, *etc* (Ding et al., 2016; Tang et al., 2018; Tao et al., 2017; Bhowmick et al., 2017; Zhu et al., 2019; Park et al., 2018; Huang et al., 2018; Rao et al., 2019; Qiao et al., 2018; Jo et al., 2017). In order to insist on the improvement of quality and novelty of our work, here

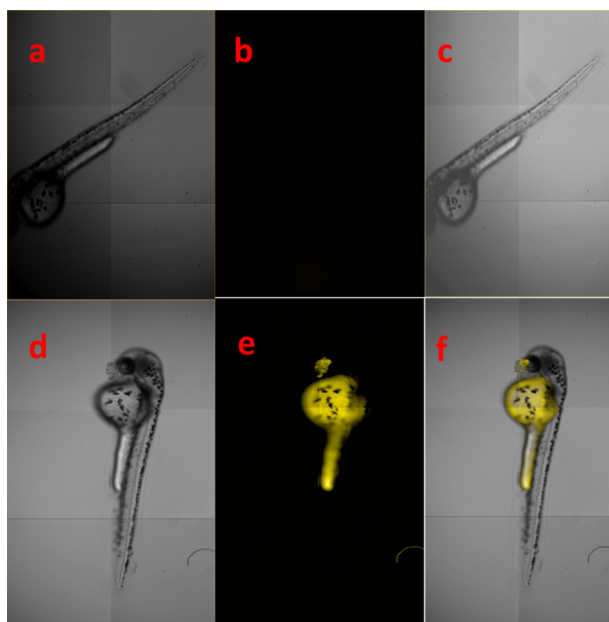


Fig. 9 Fluorescence microscopic imaging of RS (a) bright field (b) fluorescence image of chemosensor RS and (c) merged field images of bright and fluorescence field (d) bright field (e) fluorescence and (f) merged field images of Fe^{3+} ions and RS.

Table 1 Truth table for Corresponding logic circuit.

S.No	Input-1 [Fe]	Input-2 [Cu]	Output-1 A_{521}	Output-2 A_{529} (Or) I_{554}
1	0	0	0	0
2	1	0	0	1
3	0	1	1	0
4	1	1	0	1

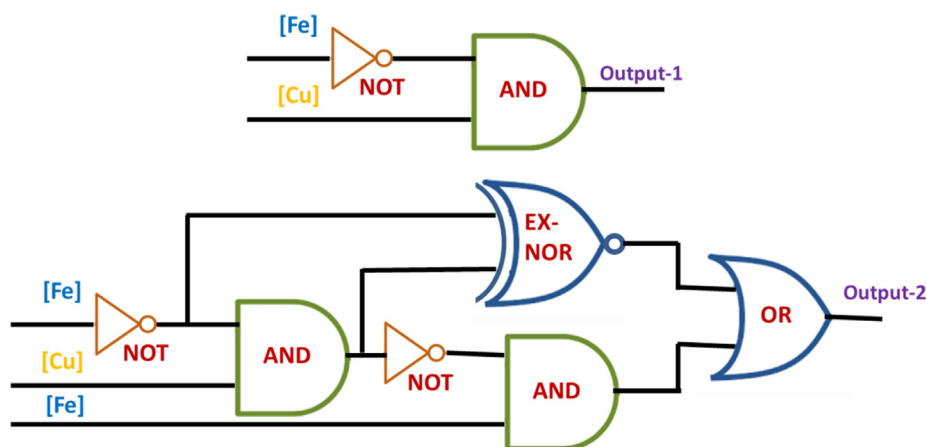


Fig. 10 Molecular logic circuit for the chemosensor RS.

we have compared with some recent reports. The simple and facile synthesized our chemosensor RS could be able to detect similar kind of two different analytes (cations) in different wavelengths for the first time ever. In addition, we have achieved ultra lowlevel sensitivity towards Fe^{3+} and Cu^{2+} ions. Though some probes existing only with rhodamine moiety were reported, such kind of distinguished detection of two paramagnetic cations by a single chemosensor is infrequent. Moreover, such previous reports did not illustrate their several applicabilities in biological aspects (Table S1). Since our chemosensor, RS is the novel one; it may be applicable as a potential sensing device for detecting Fe^{3+} and Cu^{2+} metal ions in the future.

4. Conclusions

In summary, we can say that to the best of our knowledge this is the first ideal and novel chemosensor RS, which could individually diagnose two paramagnetic ($\text{Cu}^{2+}/\text{Fe}^{3+}$) metal ions through spectral and naked eye methods with unique mechanism. The observed photochemical results reveal that the chemosensor RS showed ample affinity towards $\text{Cu}^{2+}/\text{Fe}^{3+}$ ions even in the presence of higher concentrations of various other interpreting metal ions. In addition, it has more selectivity towards Fe^{3+} ions greater than any other cations based on the competitive experiment. An excellent photo-physical property of RS was also obtained in its molecular logic gate applications by showing various logic circuits. The fluorescent bio-imaging studies notified that its negligible toxicity towards zebrafish embryos in the detection of Fe^{3+} ions. Hence, RS potentially utilized to trace out and imaging of Fe^{3+} ions in zebrafish embryos.

CRedit authorship contribution statement

A. Senthil Murugan: Conceptualization, Methodology, Software, Writing - original draft. **M. Kiruthika:** Data curation, Writing - original draft. **E.R. Abel Noelson:** Formal analysis, Investigation. **P. Yogapandi:** Formal analysis, Investigation. **G. Gnana kumar:** Formal analysis, Writing - review & editing. **J. Annaraj:** Funding acquisition, Writing - review & editing.

Declaration of Competing Interest

The authors declare the following financial interests/personal relationships which may be considered as potential competing interests: [Here we protract chemosensor for both $\text{Cu}^{2+}/\text{Fe}^{3+}$ ion pair detection with very low detection limit using rhodamine moiety with the different wavelength in absorbance spectroscopic method. This is the first report for distinguish the two paramagnetic metal ions in absorbance spectroscopy. Our synthesized chemosensor may be utilized for real time applications like biological systems. Hence, this work has much novelty and the material will become a valid tool kit for analytical method in real time analysis.].

Acknowledgements

The author A.S.M. gratefully acknowledges University Grants Commission (UGC), New Delhi for financial support in the form of Non-NET fellowship.

Appendix A. Supplementary material

Supplementary data to this article can be found online at <https://doi.org/10.1016/j.arabjc.2020.11.016>.

References

- Bannister, W.H., 1991. The biological chemistry of the elements: the inorganic chemistry of life: by J J R Fraústo da Silva and R J P Williams. Clarendon Press, Oxford, p. 561.
- Bao, G., Wong, K.-L., Tanner, P.A., 2019. A Reversible Rhodamine B Based pH Probe with Large Pseudo-Stokes Shift. *ChemPlusChem* 84, 816–820.
- Barnham, K.J., Masters, C.L., Bush, A.I., 2004. Neurodegenerative diseases and oxidative stress. *Nat. Rev. Drug Discovery* 3, 205–214.
- Bensasson, P.R.V., 1997. Inorganic biochemistry, an introduction. *Biochimie* 80, 347–348.
- Bhowmick, R., Islam, A.S.M., Giri, A., Katarkar, A., Ali, M., 2017. A rhodamine based turn-on chemosensor for Fe^{3+} in aqueous medium and interactions of its Fe^{3+} complex with HAS. *NewJ. Chem.* 41, 11661–11671.

- Bonda, D.J., Lee, H., Blair, J.A., Zhu, X., Perryab, G., Smith, M.A., 2011. Role of metal dyshomeostasis in Alzheimer's disease. *Metallomics* 3, 267–270.
- Brown, D.R., Kozlowski, H., 2004. Biological inorganic and bioinorganic chemistry of neurodegeneration based on prion and Alzheimer diseases. *Dalton Trans.*, 1907–1917
- Burdo, J.R., Connor, J.R., 2003. Brain iron uptake and homeostatic mechanisms: An overview. *Biometals* 16, 63–75.
- Cheng, Z.H., Li, G., Zhang, N., Liu, H.-O., 2014. A novel functionalized silver nanoparticles solid chemosensor for detection of Hg (II) in aqueous media. *Dalton Trans.* 43, 4762–4769.
- Cheredy, N.R., Suman, K., Korrapati, P.S., Thennarasu, S., Mandal, A.B., 2012. Design and synthesis of rhodamine based chemosensors for the detection of Fe³⁺ ions. *Dye Pigment.* 95, 606–613.
- Choi, Y.W., Park, G.J., Na, Y.J., Jo, H.Y., Lee, S.A., You, G.R., Kim, C., 2014. A single schiff base molecule for recognizing multiple metal ions: A fluorescence sensor for Zn(II) and Al(III) and colorimetric sensor for Fe(II) and Fe(III). *Sens. Actuators, B* 194, 343–352.
- Crichton, R.R., Dexter, D.T., Ward, R.J., 2008. Metal based neurodegenerative diseases from molecular mechanisms to therapeutic strategies *Coord. Chem. Rev.* 252, 1189–1199.
- Davies, K.M., Mercer, J.F., Chen, N., Double, K.L., 2016. Copper dyshomeostasis in Parkinson's disease: implications for pathogenesis and indications for novel therapeutics. *Clin. Sci.* 130, 565–574.
- Deng, F., Xu, Z., 2019. Heteroatom-substituted rhodamine dyes: Structure and spectroscopic properties. *Chin. Chem. Lett.* 30, 1667–1681.
- Ding, H., Zheng, C., Li, B., Liu, G., Pu, S., Jia, D., Zhou, Y., 2016. A rhodamine-based sensor for Hg²⁺ and resultant complex as a fluorescence sensor for I⁻. *RSC Adv.* 6, 80723–80728.
- Fang, Y., Zhou, Y., Li, J.-Y., Rui, Q.-Q., Yao, C., 2015. Naphthalimide-Rhodamine based chemosensors for colorimetric and fluorescent sensing Hg²⁺ through different signalling mechanisms in corresponding solvent systems. *Sens. Actuators B* 215, 350–359.
- Fatma, N., Mehata, M.S., Pandey, N., Pant, S., 2020. Flavones fluorescence-based dual response chemosensor for metal ions in aqueous media and fluorescence recovery. *J. Fluoresc.* 30, 759–772.
- Gabr, M.T., Pigge, F.C., 2017. A turn-on AIE active fluorescent sensor for Hg²⁺ by combination of 1,1-bis(2-pyridyl)ethylene and thiophene/bi thiophene fragments. *Mater. Chem. Front.* 1, 1654–1661.
- Huang, Q., Chen, Y.T., Ren, Y.W., Wang, Z.Y., Zhu, Y.X., Zhang, Y., 2018. A rapid and naked-eye visible rhodamine 6G-based chemosensor for sensitive detection of copper(II) ions in aqueous solution. *Anal. Methods* 10, 5731–5737.
- Huang, L., Hou, F., Cheng, J., Xi, P., Chen, F., Bai, D., Zeng, Z., 2012. Selective off-on fluorescent chemosensor for detection of Fe³⁺ ions in aqueous media *Org. Biomol. Chem.* 10, 9634–9638.
- Jo, T.G., Bok, K.H., Han, J., Lim, M.H., Kim, C., 2017. Colorimetric detection of Fe³⁺ and Fe²⁺ and sequential fluorescent detection of Al³⁺ and pyrophosphate by an imidazole-based chemosensor in a near-perfect aqueous solution. *Dyes Pigm.* 139, 136–147.
- Karakus, E., Uçuncu, M., Eanes, R.C., lu, M.E., 2013. The utilization of pH sensitive spirocyclic rhodamine dyes for monitoring D-fructose consumption during a fermentation process. *New J. Chem.* 37, 2632–2635.
- Kozlowski, H.A., Janicka-Klos, J., Brasun, E., Gaggelli, D., Valensin, G., 2009. Copper, iron, and zinc ions homeostasis and their role in neurodegenerative disorders (metal uptake, transport, distribution and regulation) *Coord. Chem. Rev.* 253, 2665–2685.
- Kumar, J., Bhattacharyya, P.K., Das, D.K., 2015. New dual fluorescent “on-off” and colorimetric sensor for Copper(II): Copper(II) binds through N coordination and pi cation interaction to sensor, *Spectrochim. Acta Part A: Mol. Biomol. Spectrosc.* 138, 99–104.
- Kwon, J.Y., Jang, Y.J., Lee, Y.J., Kim, K.M., Seo, M.S., Nam, W., Yoon, J., 2005. A Highly Selective Fluorescent Chemosensor for Pb²⁺. *J. Am. Chem. Soc.* 127, 10107–10111.
- Laglera, L.M., Monticelli, D., 2017. Iron detection and speciation in natural waters by electrochemical techniques: A critical review *Curr Opin. Electrochem* 3, 123–129.
- Lee, S.A., Lee, J.J., Shin, J.W., Min, K.S., Kim, C., 2015. A colorimetric chemosensor for the sequential detection of copper (II) and cysteine. *Dyes Pigments* 116, 131–138.
- J. Li, Y. Chen, T. Chen, J. Qiang, Z. Zhang, T. Wei, W. Zhang, F. Wang and X. Chen, A benzothiazole-based fluorescent probe for efficient detection and discrimination of Zn²⁺ and Cd²⁺, using cysteine as an auxiliary reagent, *Sens. Actuators, B*, 268 (2018) 446–455
- Li, G., Tang, J., Ding, P., Ye, Y., 2016. A Rhodamine-benzimidazole based chemosensor for Fe(III) and its application in living cells. *J. Fluoresc.* 26, 155–161.
- Li, J., Wang, Q., Guo, Z., Ma, H., Zhang, Y., Wang, B., Bin, D., Wei, Q., 2016. Highly selective fluorescent chemosensor for detection of Fe³⁺ based on Fe₃O₄@ZnO. *Sci. Reports* 6, 1–8.
- Li, Z., Yan, X., Huang, F., Sepehrpour, H., Stang, P.J., 2017. Near-Infrared Emissive Discrete Platinum(II) metallocycles: synthesis and application in ammonia detection. *Org. Lett.* 19, 5728–5731.
- Liu, X., Li, N., Li, M., Chen, H., Zhang, N., Wang, Y., Zheng, K., 2020. Recent progress in fluorescent probes for detection of carbonyl species: Formaldehyde, carbon monoxide and phosgene *Coord. Chem. Rev.* 404, 213109.
- Ma, C., Lin, L., Du, Y., Chen, L.-B., Luoc, F., Chen, X., 2013. Fluorescence quenching determination of iron(III) using rhodamine 6G hydrazide derivative. *Anal. Methods* 5, 1843–1847.
- McDonald, A.J., Dibble, J.P., Evans, E.G.B., Millhauser, G.L., 2014. A new paradigm for enzymatic control of α -cleavage and β -cleavage of the prion protein. *J. Biol. Chem.* 289, 803–813.
- Nayak, N., Armakovi, S., Pillai, R.R., Prasad, K.S., Armakovi, S.J., 2018. Remarkable colorimetric sensing behaviour of pyrazole-based chemosensor towards Cu(II) ion detection: synthesis, characterization and theoretical investigations. *RSC Adv.* 8, 18023–18029.
- Omarova, S., Demir, S., Andac, M., 2018. Development of a New spectrophotometric based flow injection analysis method for the determination of copper (II) *J. Taibah. Univ. Sci.* 12, 820–825.
- Park, H., An, K.-L., Naveen, M., Jun, K., Son, Y.-A., 2018. Rhodamine-based colorimetric and fluorescent chemosensors for the detection of Cu²⁺ ions and its application to bioimaging. *Bull. Korean Chem. Soc.* 39, 972–981.
- Patra, C., Bhanja, A.K., Sen, C., Ojha, D., Chattopadhyay, D., Mahapatra, A., Sinha, C., 2016. Vanillyl thioether Schiff base as a turn-on fluorescence sensor to Zn²⁺ ion with living cell imaging. *Sens. Actuators, B* 228, 287–294.
- Pithadia, A.S., Lim, M.H., 2012. Metal-associated amyloid- β species in Alzheimer's disease. *Curr. Opin. Chem. Biol.* 16, 67–73.
- Qi, X., Qian, J., Chen, T., Lu, D., Chen, B., 2017. Electrochemical Determination of Cu(II) Ions Based on Ag/Pd Alloy for Water Quality Early Warning *Int. J. Electrochem. Sci.* 12, 5511–5520.
- Qiao, R., Xiong, W.-Z., Bai, C.-B., Liao, J.-X., Zhang, L., 2018. A highly selective fluorescent chemosensor for Fe (III) based on rhodamine 6G dyes derivative. *Supramol. Chem.* 30, 911–917.
- Queirós, C., Leite, A., Couto, M.G.M., Moniz, T., Cunha-Silva, L., Gameiro, P., Silva, A.M.G., Rangel, M., 2014. Tuning the limits of pH interference of a rhodamine ion sensor by introducing catechol and 3-hydroxy-4-pyridinone chelating units. *Dye. Pigment* 110, 193–202.
- Rao, P.G., Saritha, B., Rao, T.S., 2019. Colorimetric and turn-on fluorescence chemosensor for Hg²⁺ ion detection in aqueous media. *J. Fluoresc.* 29, 353–360.
- Senthil Murugan, A., Jegan, A., Pannipara, M., Al-Sehemi, A.G., Phang, S.-M., Gnana Kumar, G., Annaraj, J., 2020. Synthesis of new Schiff's base copper conjugate for optically and electrochemically tuning of L-cysteine in cancer cells and bovine serum albumin *Sensors & Actuators: B. Chemical* 316, 128082.

- Sikdar, Anindita, Panja, Sujit Sankar, Biswas, Partha, Ro, Swapnadip, 2012. A rhodamine-based dual chemosensor for Cu(II) and Fe(III). *J. Fluoresc.* 22, 443–450.
- Singh, P., Singh, H., Bhargava, G., Kumar, S., 2015. Triple-signalling mechanisms-based three-in-one multi-channel chemosensor for discriminating Cu^{2+} , acetate and ion pair mimicking AND, NOR, INH and IMP logic functions. *J. Mater. Chem. C* 3, 5524–5532.
- Sivaraman, G., Anand, T., Chellappa, D., 2012. Turn-on fluorescent chemosensor for Zn(II) via ring opening of rhodamine spirolactam and their live cell imaging. *Analyst* 137, 5881–5884.
- Sivaraman, G., Iniya, M., Anand, T., Kotla, N.G., Sunnapu, O., Singaravadi, S., Gulyani, A., Chellappa, D., 2018. Chemically diverse small molecule fluorescent chemosensors for copper ion. *Coord. Chem. Rev.* 357, 50–104.
- Spolaor, A., Vallelonga, P., Gabrieli, J., Cozzi, G., Boutron, C., Barbante, C., 2012. Determination of Fe^{2+} and Fe^{3+} species by FIA-CRC-ICP-MS in Antarctic ice samples. *J. Anal. At. Spectrom.* 27, 310–317.
- Tang, X., Wang, Y., Han, J., Ni, L., Li, J., Zhang, H., Li, C., Qiu, Y., 2018. A novel fluorescent probe based on biphenyl and rhodamine for multi-metal ion recognition and its application. *Dalton Trans.* 47, 3378–3387.
- Tang, L., Xia, J., Zhong, K., Tang, Y., Gao, X., Li, J., 2020. A simple AIE-active fluorogen for relay recognition of Cu^{2+} and pyrophosphate through aggregation-switching strategy. *Dyes Pigm.* 178, 108379.
- Tao, J., Wang, X., Chen, X., Li, T., Diao, Q., Yu, H., Wang, T., 2017. Si-rhodamine B thiolactone: A simple long wavelength operating chemosensor for direct visual recognition of H^{2+} . *Dye. Pigment* 137, 601–607.
- Waggoner, D.J., Bartnikas, T.B., Gitlin, J.D., 1999. The role of copper in neurodegenerative disease. *Neurobiol. Dis.* 6, 221–230.
- Wang, D., Su, H., Kwok, R.T.K., Shan, G., Leung, A.C.S., Lee, M.M.S., Sung, H.H.Y., Williams, I.D., Lam, J.W.Y., Tang, B.Z., 2017. Facile synthesis of Red/NIR AIE luminogens with simple structures, bright emissions, and high photostabilities, and their applications for specific imaging of lipid droplets and image-guided photodynamic. *Therapy Adv. Funct. Mater.* 27, 1704039.
- Weizman, H., Ardon, O., Mester, B., Libman, J., Dwir, O., Hadar, Y., Chen, Y., Shanzer, A., 1996. Fluorescently-labeled ferrichrome analogs as probes for receptor-mediated, microbial iron uptake. *J. Am. Chem. Soc.* 118, 12368–12375.
- Xiao, G., Fan, Q., Wang, X., Zhou, B., 2013. Huntington disease arises from a combinatory toxicity of polyglutamine and copper binding. *Proc. Natl. Acad. Sci. U. S. A.* 110, 14995–15000.
- Yang, Y., Gao, C.-Y., Zhang, N., Dong, D., 2016. Tetraphenylethene functionalized rhodamine chemosensor for Fe^{3+} and Cu^{2+} ions in aqueous media. *Sens. Actuators B* 222, 741–746.
- Yang, Y., Gao, C.-Y., Zhang, N., Dong, D., 2016. Tetraphenylethene functionalized rhodamine chemosensor for Fe^{3+} and Cu^{2+} ions in aqueous media. *Sens. Actuators B* 222, 741–746.
- Yang, J., Li, L., Yu, Y., Ren, Z., Peng, Q., Ye, S., Li, Q., Li, Z., 2017. Blue pyrene-based AIEgens: inhibited intermolecular π - π stacking through the introduction of substituents with controllable intramolecular conjugation, and high external quantum efficiencies up to 3.46% in non-doped OLEDs. *Mater. Chem. Front.* 1, 91–99.
- Yang, M., Ma, L., Li, J., Kang, L., 2019. Fluorescent probe for Cu^{2+} and the secondary application of the resultant complex to detect cysteine. *RSC Adv.* 9, 16812–16818.
- Yang, Z., She, M., Yin, B., Cui, J., Zhang, Y., Sun, W., Li, J., Shi, Z., 2012. Three Rhodamine-Based “Off-On” Chemosensors with High Selectivity and Sensitivity for Fe^{3+} Imaging in Living Cells. *J. Org. Chem.* 77 (2), 1143–1147.
- Yin, W., Cui, H., Yang, Z., Li, C., She, M., Li, J., Zhao, G., Shi, Z., Yin, B., 2011. Facile synthesis and characterization of rhodamine-based colorimetric and “off-on” fluorescent chemosensor for Fe^{3+} . *Sens. Actuators B* 157, 675–680.
- Zhao, Q., Tao, G., Ge, C., Cai, Y., Qiao, Q., Jia, X., 2018. Ultrasensitive fluorescent probe for copper ion based on cadmium selenide/cadmium sulfide quantum dots capped with dimercaprol. *Spectrosc. Lett* 51, 216–222.
- Zhao, M., Yang, X.-F., He, S., Wang, L., 2009. A rhodamine-based chromogenic and fluorescent chemosensor for copper ion in aqueous media. *Sens. Actuators B* 135, 625–631.
- Zhu, X., Duan, Y., Li, P., Fan, H., Han, T., Huang, X., 2019. A highly selective and instantaneously responsive Schiff base fluorescent sensor for the “turn-off” detection of iron(III), iron(II), and copper (II) ions. *Anal. Methods* 11, 642–647.
- Zhu, J., Zhang, Y., Chen, Y., Sun, T., Tang, Y., Yang, Q., Ma, D., Wang, Y., Wang, M., Huang, Y., 2017. A Schiff base fluorescence probe for highly selective turn-on recognition of Zn^{2+} . *Tetrahedron Lett* 58, 365–370.
- Zon, L.I., 1999. Zebrafish: a new model for human disease. *Genome Res.* 9, 99–100.